

**In situ methanol adsorption on aluminum oxide monitored by a combined ORP-EIS and ATR-FTIR Kretschmann setup**

Pletincx, Sven; Fockaert, Laura Lynn I.; Meeusen, Mats; Mol, Johannes M.C.; Terryn, Herman; Hauffman, Tom

**DOI**

[10.1021/acs.jpcc.8b06806](https://doi.org/10.1021/acs.jpcc.8b06806)

**Publication date**

2018

**Document Version**

Final published version

**Published in**

Journal of Physical Chemistry C

**Citation (APA)**

Pletincx, S., Fockaert, L. L. I., Meeusen, M., Mol, J. M. C., Terryn, H., & Hauffman, T. (2018). In situ methanol adsorption on aluminum oxide monitored by a combined ORP-EIS and ATR-FTIR Kretschmann setup. *Journal of Physical Chemistry C*, 122(38), 21963-21973. <https://doi.org/10.1021/acs.jpcc.8b06806>

**Important note**

To cite this publication, please use the final published version (if applicable). Please check the document version above.

**Copyright**

Other than for strictly personal use, it is not permitted to download, forward or distribute the text or part of it, without the consent of the author(s) and/or copyright holder(s), unless the work is under an open content license such as Creative Commons.

**Takedown policy**

Please contact us and provide details if you believe this document breaches copyrights. We will remove access to the work immediately and investigate your claim.

***Green Open Access added to TU Delft Institutional Repository***

***'You share, we take care!' - Taverne project***

**<https://www.openaccess.nl/en/you-share-we-take-care>**

Otherwise as indicated in the copyright section: the publisher is the copyright holder of this work and the author uses the Dutch legislation to make this work public.

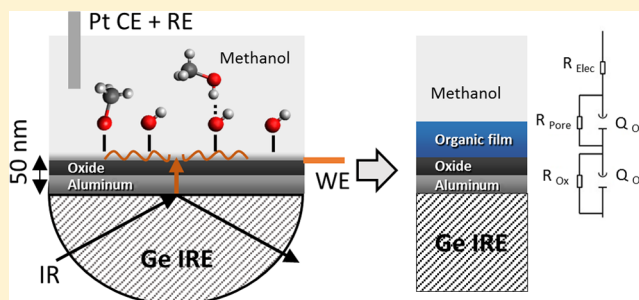
# In Situ Methanol Adsorption on Aluminum Oxide Monitored by a Combined ORP-EIS and ATR-FTIR Kretschmann Setup

Sven Pletincx,<sup>†</sup> Laura-Lynn I. Fockaert,<sup>‡</sup> Mats Meeusen,<sup>‡</sup> Johannes M. C. Mol,<sup>†</sup> Herman Terryn,<sup>†</sup> and Tom Hauffman<sup>\*,†</sup>

<sup>†</sup>Department of Electrochemical and Surface Engineering (SURF), Vrije Universiteit Brussel, Pleinlaan 2, 1050 Brussels, Belgium

<sup>‡</sup>Department of Materials Science and Engineering, Delft University of Technology, Mekelweg 2, 2628 CD, Delft, The Netherlands

**ABSTRACT:** A common approach to investigate chemical interactions at the polymer/metal oxide interface is by monitoring ultrathin polymer films onto a metal oxide substrate by a variety of surface analysis techniques. The deposition of this nanometer-thin overlayer is frequently carried out by reactive adsorption from dilute polymer solutions. However, the influence of the solvent on the metal oxide chemistry is seldom taken into account in interface studies. The overall amount of available adsorption sites on the metal oxide surface might decrease due to competing adsorption of the solvent and the polymer adsorbate. Therefore, in this work, the adsorption of a common organic solvent (methanol) onto a physical vapor-deposited aluminum oxide surface is monitored in situ by an integrated attenuated total reflectance Fourier transform infrared spectroscopy in the Kretschmann geometry and odd random phase multisine electrochemical impedance spectroscopy system. It is shown that methanol immediately physisorbs onto the aluminum oxide surface and replaces the initial adventitious carbon layer. This process is followed by methanol chemisorbing onto the oxide surface to form methoxide species at the liquid/solid interface. Additionally, chemisorption is validated ex situ by X-ray photoelectron spectroscopy.



## INTRODUCTION

Polymer/metal oxide composites play an important role in a wide range of areas such as corrosion protection, packaging, lithography, adhesion, coating application, and many others. Obtaining a fundamental understanding of bond formation and degradation mechanisms at the polymer/metal oxide interface is a necessary step to understand the overall durability of the entire composite system. The recent development of new experimental approaches enables the characterization of this region under humid or corrosive conditions.<sup>1</sup> This solid/solid interface is often referred to as the buried interface since it is not readily accessible by common surface analysis techniques. Therefore, investigating this region requires the use of a model system and a well-chosen methodology.<sup>2</sup> A common approach to gain access to this region is the use of a thin-film deposition, where the polymer film is made sufficiently thin, only a couple of nanometers, to be able to study the interaction of functional groups on metal (hydr)oxide surfaces. The deposition of this thin film is performed by dip- or spin-coating a highly diluted polymer solution, leading to organic films with a thickness of the order of nanometers.<sup>3–7</sup>

These diluted polymer solutions mainly consist of organic solvents, and for acrylic polymers, this is commonly an alcohol.<sup>8</sup> Fowkes et al. and Abel et al. previously showed that the nature of the solvent has an influence on the amount of polymer deposited on the substrate surface and that the solvent's acid–base properties govern the adsorption process

in general.<sup>9,10</sup> But despite the large abundance of the solvent molecules in contact with the oxide surface, the influence of the solvent itself on the oxide chemistry is often neglected. However, it is important to monitor the dynamics between the solvent and the metal oxide surface as the solvent can also undergo acid–base interactions with the metal oxide.<sup>11–15</sup> Due to the dynamic nature of this process, the application of an in situ technique is essential.

When previously investigating the chemical behavior of carboxylic functional groups with the aluminum (hydr)oxide surface, by monitoring the adsorption of polyacrylic acid films, an ester-functional group was observed in the C 1s spectrum.<sup>4</sup> However, this peak could not be assigned to a functional group originating from the polymer configuration. In previous investigations concerning the interfacial interactions between acrylic polymers and metal oxides, the same observation was made. Leadley et al.<sup>16</sup> proposed that the X-ray source of the X-ray photoelectron spectroscopy (XPS) and the resulting photoelectrons resulted in sample degradation, leading to the presence of ester groups. Alexander et al.<sup>17</sup> also observed this ester contribution but questioned that this functionality results from X-ray-induced damage of the thin films. They suggested that the origin of these groups may relate to the increased

Received: July 16, 2018

Revised: August 28, 2018

Published: September 4, 2018

concentration of end group functionalities in the material. However, this also seems unlikely as the observed ester contribution is rather large and the end groups make up only a small percentage of the entire polymer chain. In our previous investigation, we also considered the influence of the photon flux, but no changes in the C 1s peak were observed after continuous irradiation of the sample. Therefore, the presence of this ester group has to be explained by another process.

Ex situ and conventional attenuated total reflectance infrared spectroscopy (ATR-IR) was used to investigate the catalytic properties of alumina in contact with alcohols over a wide temperature range.<sup>11–15</sup> The collective results obtained in the field of catalysis show that methanol and ethanol form (m)ethoxide surface species onto the aluminum oxide surface at room temperature. However, also in the field of adhesion science, the characterization of the solvent/metal oxide interactions is necessary, since available bonding sites on the metal oxide surface might become occupied. A competition between the organic coating and the used solvent might lead to a decrease in overall adhesion.

Recently, the combination of both IR and impedance spectroscopy to create an integrated spectroelectrochemical system has gained interest. For example, the groups of Persson<sup>18</sup> and Grundmeier<sup>19</sup> developed novel approaches to study water diffusion through polymer coatings. Vlasak et al.<sup>20</sup> used conventional attenuated total reflectance Fourier transform infrared (ATR-FTIR) and electrochemical impedance spectroscopy (EIS) to study water uptake of thin polymer films. Öhman et al.<sup>18,21,22</sup> specifically focused on IR in the Kretschmann geometry to study the interfacial behavior of water at the solid/solid interface, combining this approach with impedance spectroscopy, which is a conventional technique that is commonly used to monitor water transport through polymer coatings as well as deterioration and/or corrosion onset in polymer/metal oxide systems.

Later, Hauffman et al.<sup>23</sup> showed the dynamic interaction behavior between ethanol and aluminum oxide in situ by introducing odd random phase multisine electrochemical impedance spectroscopy (ORP-EIS). This technique enables the possibility of a dynamic study due to shortened measurement time, and it also provides statistical information on the measurement and fitting quality. This is achieved by utilizing a random phase multisine excitation signal that contains only odd harmonics. It has been shown previously that during one single ORP-EIS experiment, the impedance, the level of the measurement noise, the level of the nonlinear distortions, and the level of nonstationary behavior are measured at each frequency and can be quantified.<sup>24</sup> From this approach, it is possible to make an evaluation of the linear and stationary behavior of the system under investigation. Another advantage is that the quantification of the noise levels allows to compare these noise data with the residuals of the fitted model, providing a way to validate the fitting quality of the selected model.<sup>25–27</sup>

In this work, the adsorption behavior between methanol and aluminum oxide is monitored as a function of time using a new spectroelectrochemical setup, based on IR in the Kretschmann geometry and ORP-EIS instead of conventional EIS, which was introduced by Öhman et al.<sup>18,21,22</sup> We investigate the origin of the earlier observed ester group XPS peak, whether this is the result of chemical interaction at the liquid/solid interface. The chemical interactions at the solvent/metal oxide interface and the subsequent organic layer formation are monitored over

time. This is done by recording information on the formed chemical bonds at the interface while in the same time frame performing an electrochemical characterization.

ATR-FTIR in the Kretschmann geometry provides an interface-sensitive and in situ analysis of a solvent/metal oxide interface. This is achieved by utilizing an internal reflecting element that is coated with a thin evaporated metal film. Nevertheless, the strong absorbing character of metals towards infrared light, an electric field can still pass through a nanometer-thin metal film. This allows the evanescent field to pass through the evaporated metal film and thus to obtain an infrared spectrum from the metal oxide/interface region. The absorption of the incident infrared light at a given wavelength represents specific interatomic interactions, and since the interface region is probed, this directly leads to information on the interfacial bonding. Simultaneously, ORP-EIS results in the characterization of the electrochemical properties of the whole system, such as the (de)adsorption of organic species or changes in the chemical structure of the oxide layer, such as the onset of corrosion processes. Therefore, this integrated approach is an excellent way to characterize the effect of the solvent on the metal oxide surface in situ at the liquid/solid interface.

## ■ EXPERIMENTAL SECTION

Attenuated total reflectance Fourier transform infrared (ATR-FTIR) spectroscopy measurements in a Kretschmann geometry were carried out by coating a germanium internal reflection element (IRE) crystal with pure aluminum (99.99% metals basis, Johnson Matthey) by means of a high-vacuum evaporation coating system (VCM 600 Standard Vacuum Thermal Evaporator, Norm Electronics). The film thickness was 50 nm, as determined by a quartz crystal microbalance. The metal film was exposed to the ambient environment to form a passivated oxide layer. During this exposure, adventitious carbon from the atmosphere unavoidably adsorbs on the metal oxide surface. The exact composition of this carbon layer is not fully understood both in this work and in the literature; however, it has been shown that it mainly consists of a combination of hydrocarbons and small carboxylic acid-based molecules.<sup>28–30</sup> The probing depth of ATR-FTIR in the Kretschmann geometry depends on the thickness of the deposited metal film and the utilized angle. A physical vapor deposition (PVD) film thickness of about 50 nm and a grazing angle are used. The evanescent wave of infrared light is largely absorbed by the deposited metal film; therefore, it is just able to reach the liquid/metal oxide surface. This leads to a probing depth of the order of nanometers and results in a near-interface spectrum (Figure 1). A more detailed description of this technique is given by Öhman et al.<sup>21</sup>

A Thermo-Nicolet Nexus FTIR apparatus equipped with a mercury–cadmium–telluride liquid-nitrogen-cooled detector and a nitrogen-purged measurement chamber with a VeeMAX III ATR accessory was used. The resolution of the acquired spectra is 4 cm<sup>-1</sup>. Spectra acquisition was controlled by the OMNIC 8.1 software package (Thermo Electron Corporation, Madison, WI). On top of the native oxide film, the electrolyte solution was placed in a sealed electrochemical cell from PIKE Technologies to measure the adsorption in situ at the interface. A spectrum of the IRE crystal coated with aluminum oxide within 3 min after contact with the electrolyte was taken as a background.

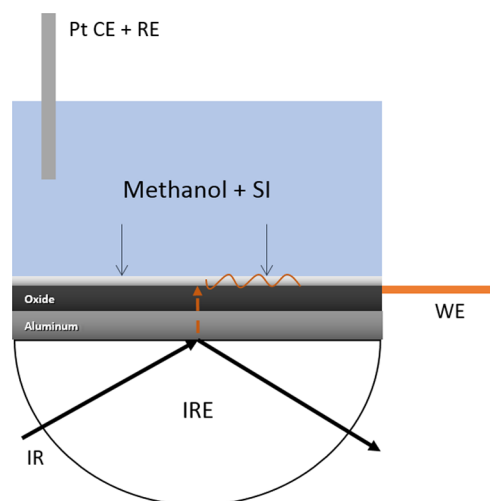


**Figure 1.** Schematic representation of the integrated impedance/infrared spectroscopy setup. A germanium crystal is coated with a 50 nm aluminum film, which is exposed to ambient conditions to form a native oxide layer, and this metal film is the working electrode. The crystal is brought into contact with a 0.1 M perchlorate methanolic solution. A platinum wire was used as a counter electrode.

Impedance spectra were acquired simultaneously by a two-electrode setup using a Biologic SP-200 potentiostat and a National Instruments PCI-4461 DAQ-card, with a platinum wire as the counter electrode (and short-circuited as pseudoreference electrode) and the deposited aluminum oxide acting as the working electrode. The electrolyte consisted of a 0.1 M  $\text{NaClO}_4 \cdot (\cdot\text{H}_2\text{O})$  (analytical grade, VWR Chemicals) methanolic solution (high-performance liquid chromatography grade,  $\geq 99.9\%$ , Sigma-Aldrich). The odd random phase

multisine perturbation signal applied was a 10 mV root mean square (RMS) variation around the open-circuit potential, consisting of the sum of harmonically related sine waves with the same amplitude and random phases. The odd harmonics are excited, and in a group of three consecutive harmonics, one harmonic is randomly omitted. Both potential and current signals are monitored at all measured frequencies (excited and nonexcited). The technique has been described in detail elsewhere.<sup>25,31,32</sup> The signal was digitally composed with MATLAB R2013a software (MathWorks Inc.), and MATLAB was also used to control the DAQ-card and to process the collected data. The impedance spectrum was acquired every 600 s between 0.01 and 2000 Hz.

X-ray photoelectron spectroscopy (XPS) images were recorded using a PHI5600 photoelectron spectrometer (Physical Electronics) with an Al  $K\alpha$  monochromatic X-ray source (1486.71 eV photon energy). The vacuum in the analysis chamber was  $5 \times 10^{-9}$  Torr or lower during measurements. High-resolution scans of the Al 2p, O 1s, and C 1s core electron peaks were recorded from a spot diameter of 0.8 mm. A pass energy of 23.5 eV and an energy step size of 0.1 eV were used. XPS data were analyzed using PHI MultiPak software (v9.5). The energy scale of the XPS images was calibrated relative to the binding energy of adventitious hydrocarbons (C–C/C–H) in the C 1s peak and set to 284.4 eV.

## RESULTS AND DISCUSSION

**Integrated Setup: Odd Random Phase Multisine EIS/FTIR in the Kretschmann Configuration.** *Infrared Spectroscopy in the Kretschmann Geometry.* Since the used background spectrum for the infrared spectroscopy measurements is the metal oxide surface just after initial exposure to

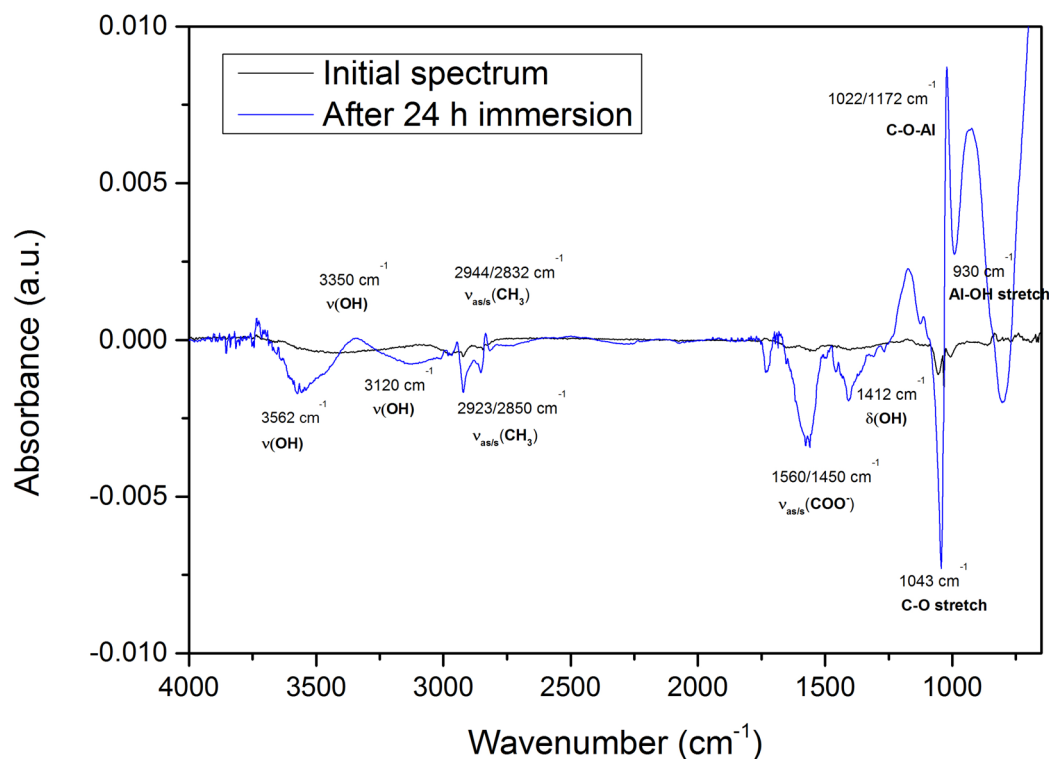


**Figure 2.** ATR-FTIR Kretschmann spectra of the methanol/aluminum oxide interface just after immersion in the methanol solution and after 24 h of immersion in the solvent. Wavenumbers ( $\text{cm}^{-1}$ ) of the major peaks are shown, combined with their respective molecular vibration.

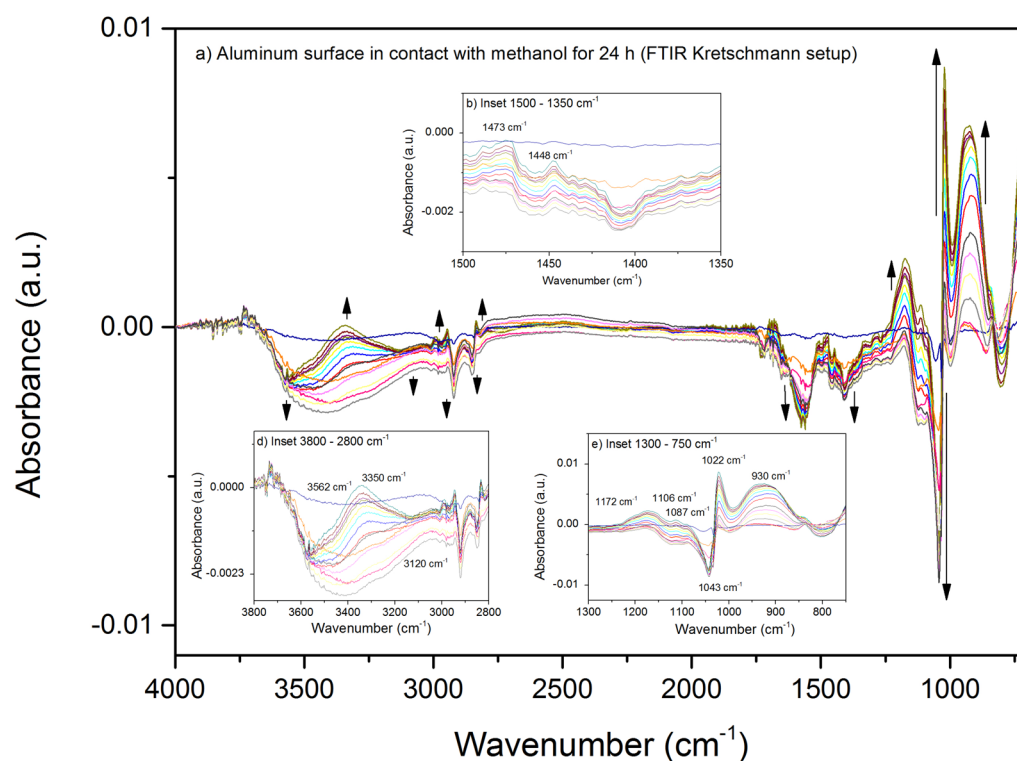


**Figure 3.** Evolution of ATR-FTIR Kretschmann spectra of the methanol/aluminum oxide interface during 24 h of immersion in the solvent (a). The negative peaks show the replacement of physisorbed methanol and adventitious carbon at the interface. The positive peaks show the formation of surface species and continuation of hydroxylation of the aluminum oxide surface. The insets show the spectra in more detail in the range of 1500–1350  $\text{cm}^{-1}$  (b), 3800–2800  $\text{cm}^{-1}$  (c), and 1300–750  $\text{cm}^{-1}$  (d).

the methanol electrolyte, the recorded spectra represent all of the changes with respect to (w.r.t.) this initial moment of exposure. This approach allows to distinguish between the species being formed at the interface (resulting in positive peaks) and the species that disappear from the interface (leading to negative peaks). By using the initial aluminum oxide/methanol electrolyte spectrum as a background, this also allows to filter out the influence of the bulk methanol electrolyte. This is shown in Figure 2, where the spectrum just after methanol immersion and the spectrum after 24 h of immersion are shown.

Figure 3 shows the evolution of the spectra at the interface between the PVD-deposited aluminum oxide layer in contact with liquid methanol every 1.5 for 24 h. During the first 250 min of exposure, mainly negative peaks are observed. These peaks correspond to physisorbed methanol and the adventitious carbon layer that are being replaced. This can be observed from the presence of the band at 1412  $\text{cm}^{-1}$ , which corresponds to the absorption band attributed to OH bending in H-bonded  $\text{CH}_3\text{OH}$ .<sup>33</sup> The negative peaks observed at 3562 and 3120  $\text{cm}^{-1}$  correspond to the OH band of water and physisorbed methanol, respectively.<sup>34</sup> The peaks at 2923 and 2850  $\text{cm}^{-1}$  correspond to the  $\text{CH}_3$  stretching vibrations of the liquid  $\text{CH}_3\text{OH}$ .<sup>11</sup> The main negative peak that is observed is the peak at 1043  $\text{cm}^{-1}$ , which represents the stretching band of the C–O bond originating from physisorbed methanol.<sup>11</sup>

Peaks are observed at 1560 and 1450  $\text{cm}^{-1}$ , which are assigned to symmetric and asymmetric carboxylate ( $\text{COO}^-$ ), showing that an initial contamination layer of adventitious carbon exists. The vapor deposition process results in a nanometer-thin film that becomes exposed to air, to form a passivated native oxide layer. During this exposure, adventi-

tious carbon adsorbs instantaneously on the metal surface.<sup>28,29</sup> van den Brand et al. showed, by means of infrared reflectance absorbance spectroscopy, that immediately upon exposure to ambient conditions, a combination of hydrocarbons and small carboxylic acid-based molecules adsorbs on the aluminum oxide surface. This was observed by the presence of symmetric and asymmetric carboxylate IR peaks in the range of 1390–1630  $\text{cm}^{-1}$ . It is also in this range that we observe the growth of these negative peaks, indicating that an adventitious carbon layer was present after the PVD process and is being replaced at the interface by the organic solvent.<sup>30</sup>

Obtaining an IR spectrum of the surface contamination layer with ATR-FTIR in the Kretschmann configuration, to analyze the exact composition of the adventitious carbon layer, is not possible since a background spectrum of the PVD film without the adventitious contamination layer cannot be recorded without the need of a cleaning step. Since this procedure is commonly the immersion of the metal oxide in an organic solvent, the use of a cleaning step was skipped to not alter the aluminum oxide surface. The initial presence of this layer only becomes apparent in the IR spectra by the growth of negative peaks in time of the  $\text{COO}^-$  bands and this after bringing the PVD-deposited layer in contact with methanol.

The positive peaks correspond to aluminum methoxide being formed at the interface. Peaks at 2944 and 2832  $\text{cm}^{-1}$  show the  $\text{CH}_3$  stretching vibrations of the methoxide. These values correspond well with the earlier observed wavenumbers of adsorbed alcohols.<sup>11,35</sup> These wavenumbers are typically shifted from the ones observed in the spectrum of liquid methanol. This is explained by the effect of the increased force constant of the CH bond of the methyl group induced by the electronegativity of the aluminum oxide.<sup>36</sup>

Table 1. Comparison of Observed in Situ Infrared Values with ex Situ Literature Data

		in situ FTIR Kretschmann ( $\text{cm}^{-1}$ ) <sup>a</sup>	ex situ FTIR (literature) ( $\text{cm}^{-1}$ ) <sup>b</sup>
physisorbed MeOH/water	OH band	3562 (-)	3335/1420
		3120 (-)/1412 (-)	
		3350 (+)	
methoxide	CH <sub>3</sub> stretching	2944 (+)	2950
		2923 (-)	
physisorbed MeOH		2832 (+)	2840
		2850 (-)	
adventitious carbon/physisorbed MeOH	C–H and COO <sup>-</sup>	1560 (-)	broad band at 1430
		1450 (-)	
		1400 (-)	
methoxide	C–O bond	1043 (-)	1030
	CH <sub>3</sub> O–Al	1172 (+)	1190
		1106 (+)	1100
		1087 (+)	1070 (expected but not observed by Greenler et al.)
	C–O bond	1022 (+)	1040
aluminum hydroxide	Al–O(H)	930 (+)	935

<sup>a</sup>Positive peaks (+); negative peaks (-). <sup>b</sup>Greenler et al.<sup>11</sup>

The infrared peaks observed at 1172, 1106, 1087, and 1022  $\text{cm}^{-1}$  can all be attributed to aluminum methoxide as was shown by Greenler et al.<sup>11</sup> However, during the ex situ experiments by Greenler et al., the peak at 1070  $\text{cm}^{-1}$  was observed from the IR spectrum of pure aluminum methoxide compound ( $\text{Al}(\text{CH}_3\text{O})_3$ ), but was not observed in their ex situ adsorption experiments. By utilizing the Kretschmann geometry, it is possible to in situ observe the growth of these peaks, and also the one that is expected near 1070  $\text{cm}^{-1}$ , which is observed at 1087  $\text{cm}^{-1}$ .

The IR peak at 930  $\text{cm}^{-1}$  is allocated to the Al–OH bond from aluminum hydroxide. This peak increases over exposure time, which can be explained either because a small amount of water is present in the used methanol solution or due to water formation at the interface.<sup>37–39</sup> This small water content leads to a further hydroxylation of the metal oxide surface. The bulk response of the water molecules is not observed as it is filtered out by the used background.

With increasing immersion time, a new peak is observed in the OH band. This peak (3350  $\text{cm}^{-1}$ ) can also be explained by the formation of water at the interface or originates from the hydroxylation of the aluminum oxide surface. Previous investigations already suggested that methanol reacts with surface hydroxyl groups of the metal oxide to form water.<sup>15,40</sup>

In Table 1, the obtained in situ data are compared to the ex situ data recorded by Greenler et al. This comparison shows the benefit of utilizing infrared spectroscopy in the Kretschmann geometry for interfacial analysis as it provides an IR spectrum of the interface region and allows for in situ studies to be performed.

*Odd Random Phase Multisine Electrochemical Impedance Spectroscopy.* In Figure 4, the Bode plots of the aluminum oxide submerged in methanol solution are shown. An evolution during the first 24 h is observed. More specifically, an increase in the magnitude of the impedance modulus in the frequency ranges of  $10^{-2}$ –1 and 1–10 Hz is observed in Figure 4a, as indicated by the two arrows. The phase plots (Figure 4b) exhibit a shift in phase toward the high-frequency range, illustrated by the arrow on the right. Also an increase in the phase angle can be observed between  $10^{-2}$  and 1 Hz, indicated by the arrow on the left.

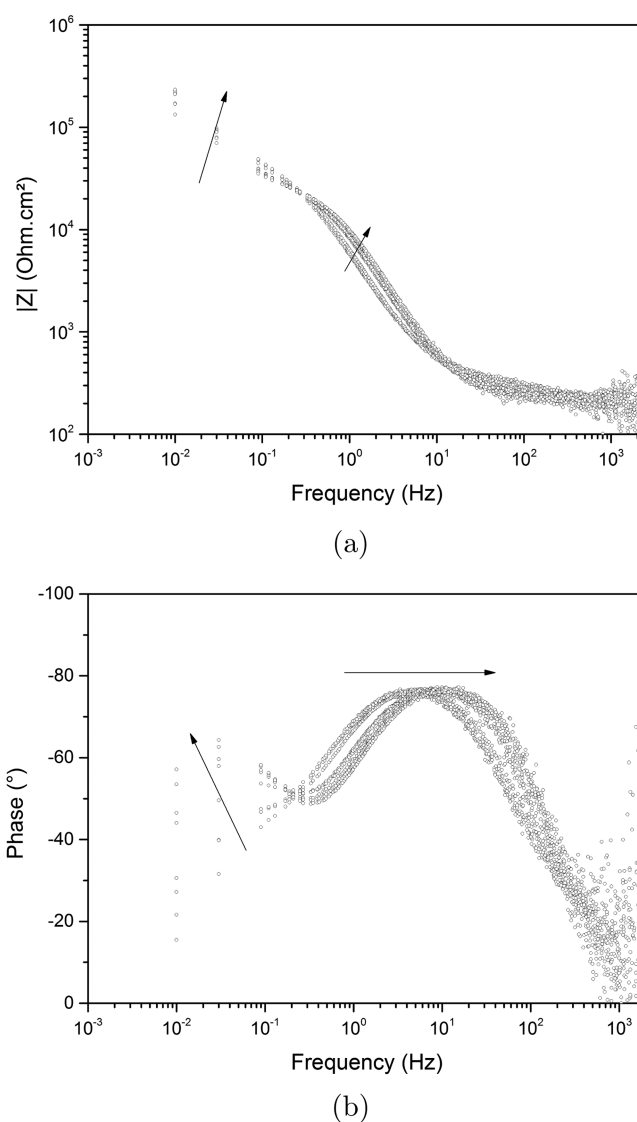
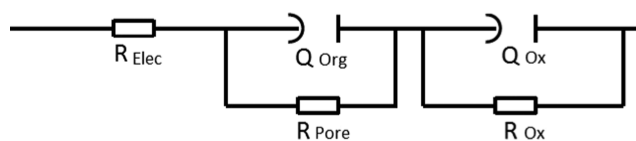


Figure 4. Bode plots of methanol adsorption onto a physical vapor-deposited aluminum oxide. Evolution during the first 24 h for (a) impedance modulus and (b) phase angle.

By analyzing ORP-EIS results, an evaluation can be made of the quality of the impedance measurements itself and about the validity of the used electric equivalent circuit (EEC), which is used to physically describe the electrochemical response of the system under investigation.<sup>26</sup> As was stated by Macía et al.,<sup>41</sup> the validity of the model can be evaluated if the following three conditions are met: (1) the model is physically meaningful, (2) the modeling residual is situated near the experimental noise level, and (3) the fitted electrochemical parameters are physically meaningful and have a low standard deviation. The validity of the model by monitoring these conditions is discussed further.

From the phase information shown in Figure 4b, it is seen that at least two relaxation constants are present, as the phase signal varies asymmetrically. The proposed model is shown in Figure 5.

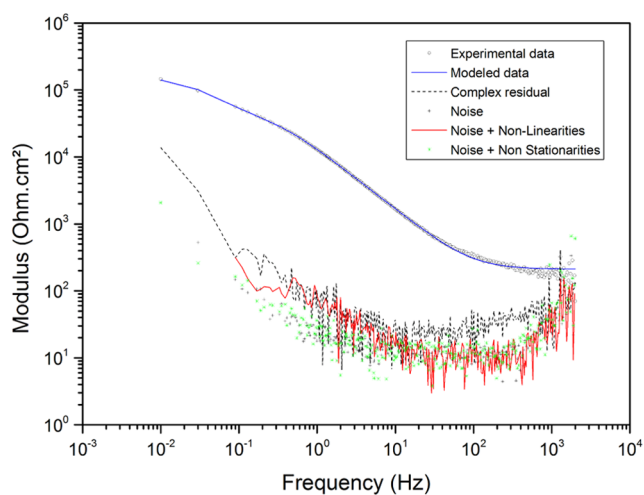


**Figure 5.** Equivalent electrical circuit for methanol adsorption on aluminum oxide. The first time constant describes the adsorption ( $R_{\text{pore}}$  and constant phase element  $Q_{\text{org}}$ ), and the second time constant describes the oxide layer ( $R_{\text{ox}}$  and constant phase element  $Q_{\text{ox}}$ ).

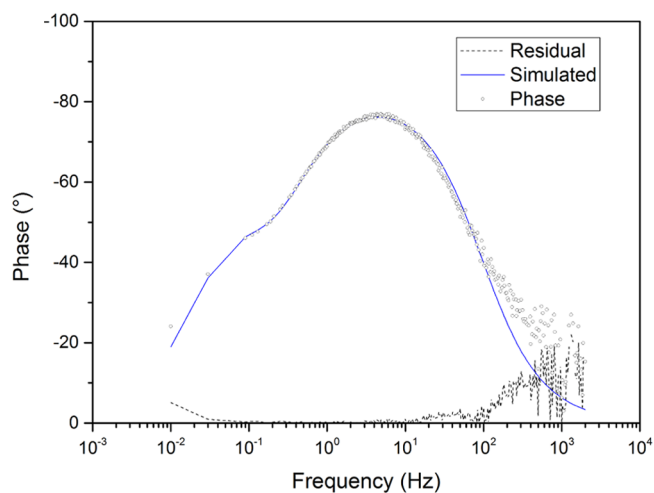
Here,  $R_{\text{elec}}$  represents the electrolyte resistance.  $R_{\text{pore}}$  and  $Q_{\text{org}}$  are the resistance and constant phase element representing the organic layer, respectively, which consists of the reactions between methanol and aluminum surface hydroxyl groups and also consists of the initial adventitious carbon layer.  $R_{\text{ox}}$  and  $Q_{\text{ox}}$  are the resistance and constant phase element mimicking the oxide layer response. The proposed EEC represents a combination of the electrolyte, the organic film, and the metal oxide and was already previously used in the literature to describe the adsorption of molecules on a metal oxide system.<sup>23,42</sup> All of the logical components that are expected to describe the system under investigation are present in this model. Therefore, and together with the earlier observations obtained from IR spectroscopy, it can be stated that the proposed model has the potential to be physically meaningful and that condition (1) has been met.

In Figure 6, the magnitude and phase Bode plots after 1 h of immersion are shown together with the modeled curve, the residual curve, the noise curve, the noise + nonlinearities curve, and the noise + nonstationarities curve. Due to the application of an odd random phase multisine input signal, it is possible to make an evaluation of the quality of the impedance measurements.<sup>25–27,41</sup> When the noise + nonlinearities curve overlaps with the noise level, the system behaves linear. If the noise level and the noise + nonstationarities curve do not differ, then the system behaves stationary. It is observed that these curves make a nearly exact overlay with the experimental noise. This shows that the system behaves both linear and stationary during the measurement and this under the given excitation amplitude of 10 mV RMS.

An evaluation of the quality of the used EEC is obtained from Figure 6, where the proposed model (Figure 5) is fitted onto the experimental data.<sup>27,43</sup> This is done by fitting the electrochemical parameters in the corresponding impedance–frequency equation of the model to the experimental data by the Levenberg–Marquardt method. By minimizing a cost



(a)



(b)

**Figure 6.** Bode amplitude (a) and phase plot (b) containing the experimental data, modeled curve, residual curve, noise curve, noise on the excited frequencies, and noise on the nonexcited frequencies of the measurement at 1 h of immersion time.

function representing the distance between model and experimental data, where the data are weighted according to the noise, best-fit parameters are obtained together with their standard deviation. The goodness of fit can be assessed by the resulting complex residual. When looking at the complex residual, which represents the difference between experimental and modeled values, it is observed that this curve is situated near the noise levels of the measurement up to  $10^3$  Hz. It is observed that from  $10^3$  Hz on, the noise level increases drastically. This is because the raw measured data are extracted from the potentiostat without any compensation procedure, which is typically built in by the manufacturer in the operating software of the potentiostat. This leads to a low signal-to-noise ratio from this frequency on. Since for the fitting procedure the data are weighted according to the noise, a deviation of the complex residual is observed in this frequency range. However, in the high-frequency region, only the influence of the electrolyte resistance is present. The fitted Bode amplitude curve still follows the experimental data, whereas only a deviation is observed in the Bode phase plot in this frequency

range. Since the complex residual relative to the impedance magnitude is low enough, with all values under 10%, condition (2) for the validity of the model can be accepted. The complex residual stays near the noise levels (with all values under 10%) for every measurement cycle; therefore, the goodness of fit is accepted for all measurements over the entire immersion time.

**Evaluation of the IR and Electrochemical Parameters as a Function of Immersion Time.** By combining odd random phase multisine electrochemical impedance spectroscopy with infrared spectroscopy in the Kretschmann geometry, it is possible to couple physically relevant information originating from the liquid/solid interface obtained by IR spectroscopy to the fitted impedance parameters.

In Figure 7, an overview of the absolute IR peak height intensities as a function of immersion time is shown. From this

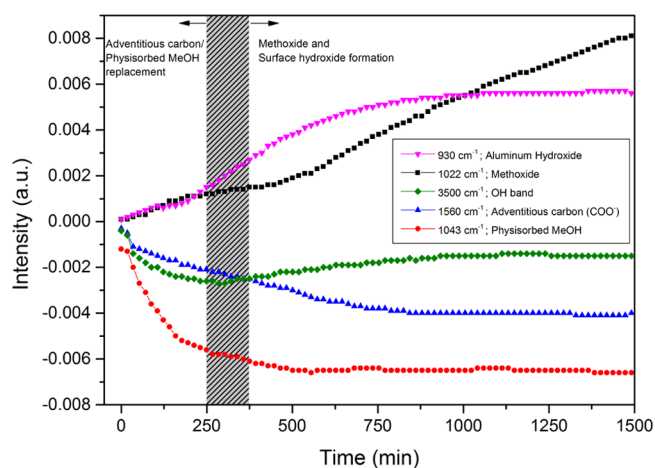


**Figure 7.** Infrared peak intensities at the liquid/solid interface as a function of immersion time in the solvent.

overview, it can be observed that the chemisorption of methanol, to form methoxide species ( $1022\text{ cm}^{-1}$ ), happens over the entire immersion time. However, it is only after the first 375 min, when the adventitious carbon layer ( $1560\text{ cm}^{-1}$ ) and the physisorbed methanol layer ( $1043\text{ cm}^{-1}$ ) have been replaced that the methoxide formation reaches a steady growth rate. When looking at the OH band ( $3500\text{ cm}^{-1}$ ), it is observed that this band first becomes more negative up to 375 min, after which it becomes more positive again. This can be explained either due to a continuous hydroxylation of the aluminum oxide surface (observed by the increase in Al–OH band at  $930\text{ cm}^{-1}$ ) or due to the formation of water by the chemisorption process.

The fitted impedance parameters, based on the EEC shown in Figure 5, and their standard deviation as a function of methanol immersion time are shown in Figure 8. The values of the EEC parameters initially, after 250 min and after 24 h of immersion are shown in Table 2. Since heterogeneous surface behavior can be expected during organic layer formation, the formula of Brug is used to calculate the effective capacitance.<sup>44</sup>

When looking at the electrolyte resistance ( $R_{\text{elec}}$ ) in Figure 8a, a decreasing trend (from  $270 \pm 10$  to  $172 \pm 6\ \Omega\text{ cm}^2$ ) as a function of time is observed. This can be explained by the volatility of the solvent. Notwithstanding excessive shielding of the electrochemical cell containing the solvent, evaporation could not be prevented. Due to very minor gaps, probably around the entrance points of the electrodes, the methanol can unavoidably evaporate. Due to the high sensitivity of the

impedance spectroscopy and the long measurement time, this change is observed. Over the entire experiment, the solution resistance changes about  $98\ \Omega\text{ cm}^2$ . When looking at the impedance study of ethanol adsorption by Hauffman et al., the change in electrolyte resistance is also about  $50\ \Omega\text{ cm}^2$  over the entire measurement duration.<sup>23</sup> Since methanol is more volatile than ethanol, the larger decrease in resistance is expected, as the concentration of the supporting ions increases over time.

During the first 250–375 min, a strong decrease in the pore resistance of the organic layer ( $R_{\text{pore}}$ ) is observed (Figure 8b). This decrease from  $28.92 \pm 0.17$  to  $20.23 \pm 0.05\ \text{k}\Omega\text{ cm}^2$  represents the replacement of the original organic layer, consisting of a physisorbed methanol film and adventitious carbon contamination. Since organic solvents are commonly used as cleaning agent to remove the adventitious contamination layer, the presented approach allows to observe the effectiveness of this cleaning procedure and to follow the contamination replacement as a function of time.<sup>45</sup> After this layer has been replaced, the pore resistance increases toward  $22.30 \pm 0.04\ \text{k}\Omega\text{ cm}^2$ , which indicates the formation of the organic layer, as the pores in the organic film become smaller. After 875 min, the pore resistance stays stable, and from that time on, a stable state is reached and the pore size of the organic film does not change.

Also in Figure 8b, an overlay of the evolution of  $R_{\text{pore}}$  and the corresponding IR peaks of the methoxide surface specie, the physisorbed methanol, and the adventitious carbon layer are shown. During these first 250–375 min of exposure, mainly negative peaks are observed from the IR spectra, showing that mainly species are being replaced at the interface. The drop in  $R_{\text{pore}}$  corresponds to the growing negative peaks of the physisorbed methanol and the adventitious carbon layer, showing that these components are being replaced. After the replacement of these two contributions, the chemisorption process occurs at a steady rate over the entire time period.

The capacitance of the organic layer ( $C_{\text{org}}$ ) shows a decreasing trend from  $11.95 \pm 0.33$  to  $6.29 \pm 0.04\ \mu\text{F}/\text{cm}^2$ . We assign this to an increase in thickness (Figure 8c). This suggests that over the entire period of 1500 min, the organic layer is growing on top of the aluminum oxide surface. This also corresponds to the increasing contribution of the methoxide peak, showing that a chemisorbed layer at the interface is being formed.

The resistance of the oxide layer ( $R_{\text{ox}}$ ) is shown in Figure 8d. Here, an increasing trend from  $162.23 \pm 22.31$  to  $985.19 \pm 177.85\ \text{k}\Omega\text{ cm}^2$  is seen over time. Since only changes are observed in the resistive behavior of the oxide, it is assumed that these changes only originate from a changing ion concentration in the oxide pores. It should also be mentioned that this parameter is typically fitted from the low-frequency region. Therefore, this parameter is less precise due to the lower signal-to-noise ratio (shown in Figure 6), which results in a larger standard deviation of this parameter.

The capacitance of the oxide layer ( $C_{\text{ox}}$ ), shown in Figure 8e, has a value of  $15.92 \pm 0.08\ \mu\text{F}/\text{cm}^2$  and remains stable over time. This indicates that the oxide layer thickness does not change over time due to the immersion.

From the discussion above, it is seen that the electrochemical parameters follow a physically meaningful trend, in accordance with the measured infrared spectra, and have reasonably low standard deviations. This indicates that condition (3) for the validity of the model is accepted.

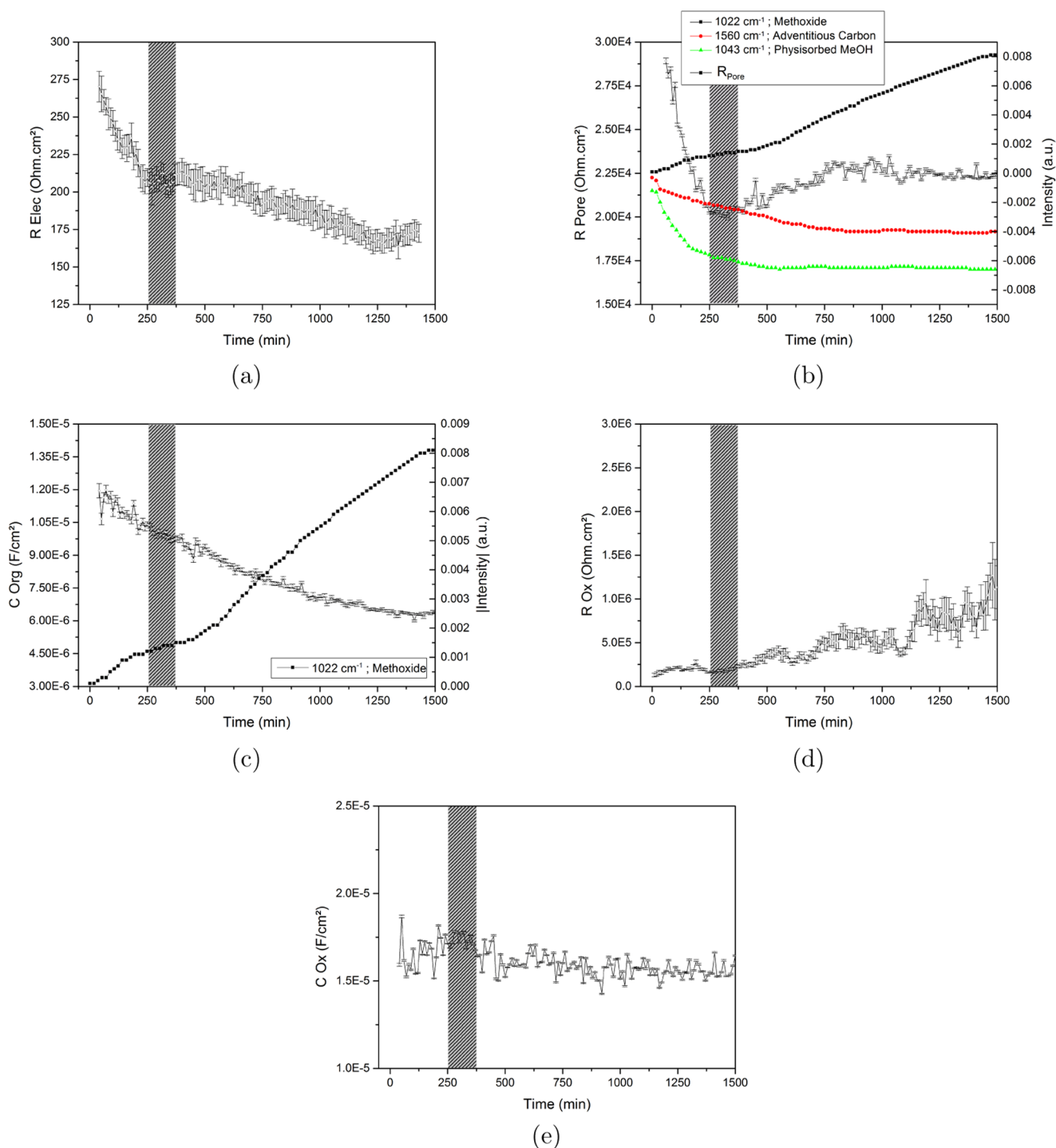


**Figure 8.** Fitted parameters and their standard deviation as a function of submersion time. (a) Electrolyte resistance ( $R_{\text{elec}}$ ); (b) pore resistance of the organic layer ( $R_{\text{pore}}$ ) and IR peak intensities of methoxide, physisorbed methanol, and adventitious carbon; (c) effective capacitance of the organic layer ( $C_{\text{org}}$ ) and IR peak intensity of methoxide surface species; (d) resistance of the oxide layer ( $R_{\text{ox}}$ ); and (e) effective capacitance of the oxide layer ( $C_{\text{ox}}$ ).

Therefore, it is shown statistically that the proposed model can describe the interactions occurring at the methanol/aluminum oxide interface. This can be concluded because of (1) the physical meaning of the model, (2) the close proximity of the modeling residual near the experimental noise level, and (3) the fitted electrochemical parameters have physical meaning and also a low standard deviation.

It is shown that the integrated setup provides complementary information of the system under investigation, which

would not be possible when only one of the two techniques would have been applied. Differentiating between multiple types of interfacial interactions at the interface is not possible with ORP-EIS, whereas these bands can easily be observed in the infrared spectra. From the ORP-EIS data, it was possible to link the decrease in capacitance of the organic layer and the changes in the pore resistance to the changes in different IR peaks, indicating chemisorption at the interface and overall organic layer growth. On the other hand, no changes in the

**Table 2. Values and Standard Deviations of the Fitted Parameters at Different Immersion Times**

parameter	initial	250 min	24 h
$R_{\text{elec}}$ ( $\Omega \text{ cm}^2$ )	$270 \pm 10$	$210 \pm 6$	$172 \pm 6$
$R_{\text{pore}}$ ( $\text{k}\Omega \text{ cm}^2$ )	$28.92 \pm 0.17$	$20.23 \pm 0.05$	$22.30 \pm 0.04$
$R_{\text{ox}}$ ( $\text{k}\Omega \text{ cm}^2$ )	$162.23 \pm 22.31$	$162.62 \pm 7.56$	$985.19 \pm 177.85$
$C_{\text{org}}$ ( $\mu\text{F}/\text{cm}^2$ )	$11.95 \pm 0.33$	$10.42 \pm 0.12$	$6.29 \pm 0.04$
$C_{\text{ox}}$ ( $\mu\text{F}/\text{cm}^2$ )	$15.92 \pm 0.08$	$17.14 \pm 0.02$	$15.27 \pm 0.03$

oxide layer capacitance are observed from the ORP-EIS data. This indicates that the oxide thickness stays constant, whereas from the infrared spectra, it is seen that the content of surface hydroxyl groups at the interface increases.

To conclude, it is shown that impedance spectroscopy is able to in situ monitor the growth of a thin organic film; however, it is not possible to distinguish the different types of chemical interactions at the liquid/solid interface from the impedance spectra alone. By combining this technique with infrared spectroscopy in the Kretschmann configuration, we obtain complementary information on the type of interfacial interactions and this as a function of time.

**X-ray Photoelectron Spectroscopy.** Figure 9 shows the C 1s XPS image of an aluminum oxide surface exposed to an ambient atmosphere compared to a surface that was immersed in methanol for 3 days.

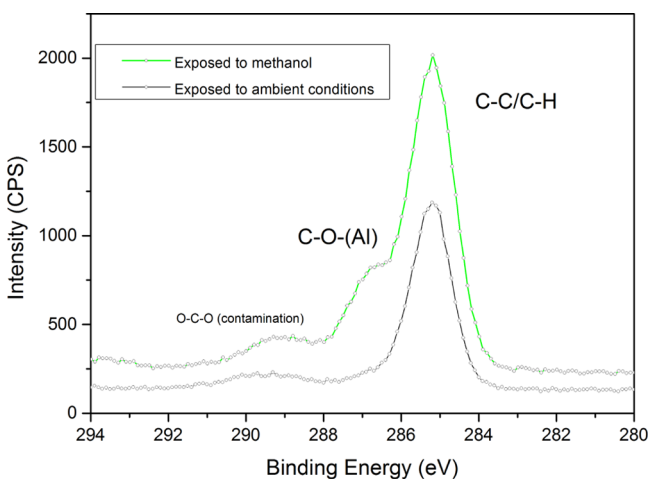


**Figure 9.** C 1s XPS images of blank aluminum oxide (black) and native aluminum oxide after 3 days of immersion in methanol (green). An extra peak at 1.9 eV (w.r.t. the C–C/C–H peak) can be observed, indicating the presence of an ether group originating from the formed methoxide surface species.

The blank aluminum oxide surface only exhibits a C–C/C–H and O–C–O peak originating from adventitious carbon on top of the substrate since the substrate is exposed to air to form the passivated oxide layer. The XPS images of the C 1s peak on the blank substrate show that the adventitious contamination layer mainly consists of a combination of hydrocarbons and small carboxylic acid–base molecules, as was shown by van den Brand et al. on aluminum oxide surfaces that are exposed to air.<sup>28,30</sup> The spectra of the exposed substrate also show the same peaks; however, an extra peak can be observed. This peak has a binding energy shift of 1.9 eV with respect to the C–C/C–H peak and corresponds to an ether peak. All of the physisorbed species would have desorbed due to the low

pressure. As this peak is observed in vacuum, it can be stated that this peak originates from chemisorbed methanol onto the aluminum oxide surface. The ether peak is observed at the same binding energy as the unknown photoelectron peak that was observed when investigating the interface of ultrathin acrylic polymers adsorbed onto a metal oxide. Therefore, we can also state that the unknown peak results from the adsorbed solvent onto the metal oxide surface.<sup>4,16,17</sup> Extra information originates from the background of the spectra where the background of the methanol-exposed substrate is higher than that of the nonexposed substrate. This shows that an organic overlayer is formed onto the methanol-exposed substrate, which leads to more elastic scattering of electrons and thus a higher background intensity.<sup>46</sup>

In Figure 10, the O 1s and Al 2p XPS images of a blank aluminum oxide exposed to ambient conditions and after 3 days of immersion in methanol are shown. From the O 1s spectra, it is seen that the peak broadens toward higher binding

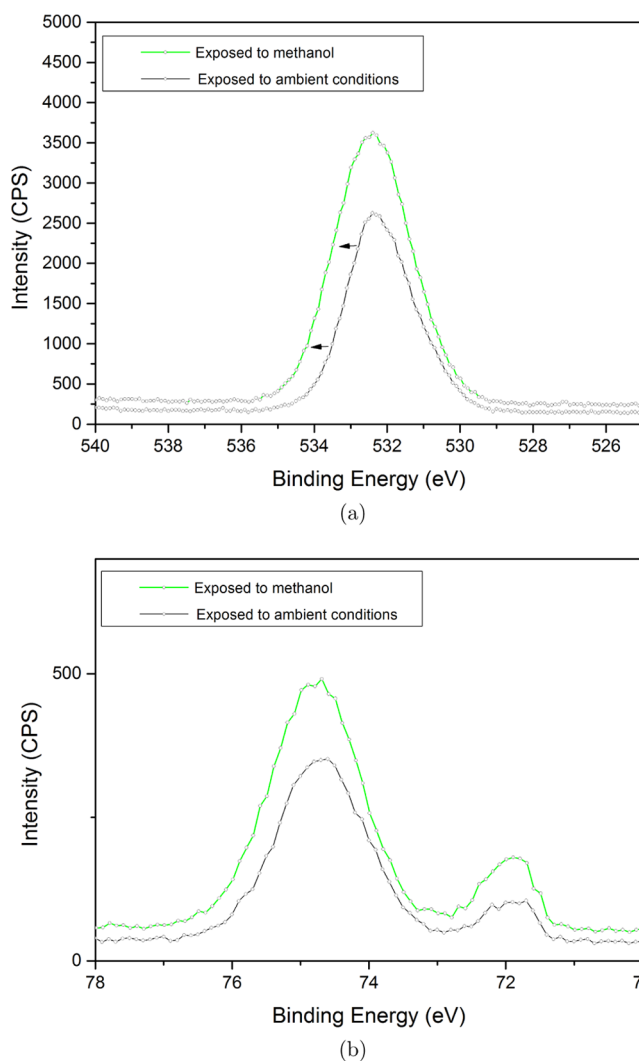


**Figure 10.** (a) O 1s XPS images and (b) Al 2p spectra of a blank aluminum oxide (black) and native aluminum oxide after 3 days of immersion in methanol (green). A broadening of the O 1s peak toward higher binding energy can be observed, indicating an increased OH contribution originating from surface hydroxyls or water. And the higher background intensity indicates the presence of an organic overlayer, which is also seen in the Al 2p spectra.

energy. This indicates an increase in the OH and C–O contribution, typically overlapping and located in this region.<sup>47</sup> The increase in C–O contribution originates from the chemisorbed methanol, whereas the OH contribution can be explained by the presence of additional surface hydroxyl groups on the aluminum oxide surface or due to the presence of water after the methanol chemisorption.<sup>48</sup> This peak broadening corresponds to the observation of increasing IR peaks assigned to OH groups and methoxide surface species. From the Al 2p XPS image, no significant changes in peak position are observed. Both spectra also show an increased background intensity w.r.t. the nonimmersed substrate, indicating the presence of an overlayer.

## CONCLUSIONS

Our investigations reported here show the chemisorption of methanol onto the aluminum oxide surface in situ. It was shown that ATR-FTIR in the Kretschmann configuration can be combined with odd random phase multisine electrochemical impedance spectroscopy to identify and monitor the formation of methoxide species at the liquid/solid interface. An electric equivalent circuit (EEC) model describing the adsorption behavior was proposed and proven statistically valid. Trends of the fitted parameters were linked to the infrared spectra, allowing to explain the EEC in a physically meaningful manner. Initially, physisorbed methanol and adventitious carbon are replaced at the interface, followed by chemisorption of methanol to form methoxide species. An increase in organic layer resistance and a decrease in its pseudocapacitance were observed and could be related to organic layer thickness growth or densification. During this process, the hydroxyl content of the aluminum oxide surface increases. This hydroxylation originates from water present in the methanol solution or due to water formation at the interface by the chemisorption reaction. Additionally, XPS was utilized to show ex situ the formation of a methoxide surface specie. It is thus important to take into account the solvent/metal oxide interactions since this interaction might lead to a decrease in available bonding sites on the metal oxide surface when depositing polymers from polymer solutions.

## AUTHOR INFORMATION

### Corresponding Author

\*E-mail: Tom.Hauffman@vub.be. Phone: 0032 2 629 35 38.

### ORCID

Sven Pletincx: 0000-0003-4070-6019

Johannes M. C. Mol: 0000-0003-1810-5145

Tom Hauffman: 0000-0002-3456-0271

### Notes

The authors declare no competing financial interest.

## ACKNOWLEDGMENTS

S.P., H.T., and T.H. acknowledge financial support by Research Foundation—Flanders (FWO) under project number SB-19-151. L.-L.I.F., M.M., and J.M.C.M. acknowledge funding under project numbers F81.6.13509 and F81.6.13503 in the framework of the Partnership Program of the Materials Innovation Institute M2i ([www.m2i.nl](http://www.m2i.nl)) and the Foundation of Fundamental Research on Matter (FOM) ([www.fom.nl](http://www.fom.nl)), which is part of the Netherlands Organisation for Scientific Research NWO ([www.nwo.nl](http://www.nwo.nl)). The authors thank Agnieszka

Kooijman, Joost van Dam, and Oscar Steenhaut for technical support in the measurements.

## REFERENCES

- (1) González-Orive, A.; Giner, I.; de los Arcos, T.; Keller, A.; Grundmeier, G. Analysis of Polymer/Oxide Interfaces under Ambient Conditions - an Experimental Perspective. *Appl. Surf. Sci.* **2018**, *442*, 581–594.
- (2) Grundmeier, G.; Stratmann, M. Adhesion and De-Adhesion Mechanisms at Polymer/Metal Interfaces: Mechanistic Understanding Based on In Situ Studies of Buried Interfaces. *Annu. Rev. Mater. Res.* **2005**, *35*, 571–615.
- (3) Pletincx, S.; Marcoen, K.; Trotochaud, L.; Fockaert, L.-L.; Mol, J. M. C.; Head, A. R.; Karşlıoğlu, O.; Bluhm, H.; Terryn, H.; Hauffman, T. Unravelling the Chemical Influence of Water on the PMMA/Aluminum Oxide Hybrid Interface In Situ. *Sci. Rep.* **2017**, *7*, No. 13341.
- (4) Pletincx, S.; Trotochaud, L.; Fockaert, L.-L.; Mol, J. M. C.; Head, A. R.; Karşlıoğlu, O.; Bluhm, H.; Terryn, H.; Hauffman, T. In Situ Characterization of the Initial Effect of Water on Molecular Interactions at the Interface of Organic/Inorganic Hybrid Systems. *Sci. Rep.* **2017**, *7*, No. 45123.
- (5) Watts, J. F.; Chehimi, M. M.; Gibson, E. M. Acid-Base Interactions in Adhesion: The Characterization of Surfaces & Interfaces by XPS. *J. Adhes.* **1992**, *39*, 145–156.
- (6) Tannenbaum, R.; King, S.; Lecy, J.; Tirrell, M.; Potts, L. Infrared Study of the Kinetics and Mechanism of Adsorption of Acrylic Polymers on Alumina Surfaces. *Langmuir* **2004**, *20*, 4507–4514.
- (7) Konstadinidis, K.; Thakkar, B.; Chakraborty, A.; Potts, L. W.; Tannenbaum, R.; Tirrell, M.; Evans, J. F. Segment Level Chemistry and Chain Conformation in the Reactive Adsorption of Poly(Methyl Methacrylate) on Aluminum Oxide Surfaces. *Langmuir* **1992**, *8*, 1307–1317.
- (8) Koo, E.; Yoon, S.; Atre, S. V.; Allara, D. L. Robust, Functionalizable, Nanometer-Thick Poly(Acrylic Acid) Films Spontaneously Assembled on Oxidized Aluminum Substrates: Structures and Chemical Properties. *Langmuir* **2011**, *27*, 3638–3653.
- (9) Abel, M. L.; Chehimi, M. M. Effect of Acid-Base Interactions on the Adsorption of PMMA on Chloride-Doped Polypyrrole from Neutral, Acidic and Basic Solvents: an XPS Study. *Synth. Met.* **1994**, *66*, 225–233.
- (10) Fowkes, F. M.; Mostafa, M. A. Acid-Base Interactions in Polymer Adsorption. *Ind. Eng. Chem. Prod. Res. Dev.* **1978**, *17*, 3–7.
- (11) Greenler, R. G. Infrared Study of the Adsorption of Methanol and Ethanol on Magnesium Oxide. *J. Chem. Phys.* **1962**, *37*, 2094–2100.
- (12) Busca, G. Infrared Studies of the Reactive Adsorption of Organic Molecules over Metal Oxides and of the Mechanisms of their Heterogeneously-Catalyzed Oxidation. *Catal. Today* **1996**, *27*, 457–496.
- (13) Kagel, R. O. Infrared Investigation of the Adsorption and Surface Reactions of the C<sub>1</sub> through C<sub>4</sub> Normal Alcohols on  $\gamma$ -Alumina. *J. Phys. Chem.* **1967**, *71*, 844–850.
- (14) Soma, Y.; Onishi, T.; Tamaru, K. Mechanism of Alcohol Decomposition over Alumina. *Trans. Faraday Soc.* **1969**, *65*, 2215–2223.
- (15) Evans, H. E.; Weinberg, W. H. The Reaction of Ethanol with an Aluminum Oxide Surface Studied by Inelastic Electron Tunneling Spectroscopy. *J. Chem. Phys.* **1979**, *71*, 1537–1542.
- (16) Leadley, S. R.; Watts, J. F. The Use of XPS to Examine the Interaction of PMMA with Oxidised Metal Substrates. *J. Electron Spectrosc. Relat. Phenom.* **1997**, *85*, 107–121.
- (17) Alexander, M. R.; Beamson, G.; Blomfield, C. J.; Leggett, G.; Duc, T. M. Interaction of Carboxylic Acids with the Oxyhydroxide Surface of Aluminium: Poly(Acrylic Acid), Acetic Acid and Propionic Acid on Pseudoboehmite. *J. Electron Spectrosc. Relat. Phenom.* **2001**, *121*, 19–32.

- (18) Öhman, M.; Persson, D. An Integrated In Situ ATR-FTIR and EIS Set-up to Study Buried Metal-Polymer Interfaces Exposed to an Electrolyte Solution. *Electrochim. Acta* **2007**, *52*, 5159–5171.
- (19) Posner, R.; Wapner, K.; Stratmann, M.; Grundmeier, G. Transport Processes of Hydrated Ions at Polymer/Oxide/Metal Interfaces. *Electrochim. Acta* **2009**, *54*, 891–899.
- (20) Vlasak, R.; Klueppel, I.; Grundmeier, G. Combined EIS and FTIR-ATR Study of Water Uptake and Diffusion in Polymer Films on Semiconducting Electrodes. *Electrochim. Acta* **2007**, *52*, 8075–8080.
- (21) Öhman, M. Development of ATR-FTIR Kretschmann Spectroscopy for in Situ Studies of Metal/Polymer Interfaces and Its Integration with EIS for Exposure to Corrosive Conditions. Ph.D. Dissertation, KTH Chemical Science and Engineering: Sweden, 2010.
- (22) Öhman, M.; Persson, D. ATR-FTIR Kretschmann Spectroscopy for Interfacial Studies of a Hidden Aluminum Surface Coated with a Silane Film and Epoxy I. Characterization by IRRAS and ATR-FTIR. *Surf. Interface Anal.* **2012**, *44*, 133–143.
- (23) Hauffman, T.; Breugelmans, T.; van Ingelgem, Y.; Tourwé, E.; Terryn, H.; Hubin, A. Measuring The Adsorption of Ethanol on Aluminium Oxides using Odd Random Phase Multisine Electrochemical Impedance Spectroscopy. *Electrochem. Commun.* **2012**, *22*, 124–127.
- (24) Van Ingelgem, Y.; Tourwé, E.; Blajiev, O.; Pintelon, R.; Hubin, A. Advantages of Odd Random Phase Multisine Electrochemical Impedance Measurements. *Electroanalysis* **2009**, *21*, 730–739.
- (25) Van Gheem, E.; Pintelon, R.; Vereecken, J.; Schoukens, J.; Hubin, A.; Verboven, P.; Blajiev, O. Electrochemical Impedance Spectroscopy in the Presence of Non-Linear Distortions and Non-Stationary Behaviour Part I: Theory and Validation. *Electrochim. Acta* **2004**, *49*, 4753–4762.
- (26) Breugelmans, T.; Tourwé, E.; Jorcin, J. B.; Alvarez-Pampliega, A.; Geboes, B.; Terryn, H.; Hubin, A. Odd Random Phase Multisine EIS for Organic Coating Analysis. *Prog. Org. Coat.* **2010**, *69*, 215–218.
- (27) Hauffman, T.; van Ingelgem, Y.; Breugelmans, T.; Tourwé, E.; Terryn, H.; Hubin, A. Dynamic, In Situ Study of Self-Assembling Organic Phosphonic Acid Monolayers from Ethanolic Solutions on Aluminium Oxides by means of Odd Random Phase Multisine Electrochemical Impedance Spectroscopy. *Electrochim. Acta* **2013**, *106*, 342–350.
- (28) Barr, T. L.; Seal, S. Nature of the Use of Adventitious Carbon as a Binding Energy Standard. *J. Vac. Sci. Technol., A* **1995**, *13*, 1239–1246.
- (29) Miller, D. J.; Biesinger, M. C.; McIntyre, N. S. Interactions of CO<sub>2</sub> and CO at Fractional Atmosphere Pressures with Iron and Iron Oxide Surfaces: One Possible Mechanism for Surface Contamination? *Surf. Interface Anal.* **2002**, *33*, 299–305.
- (30) van den Brand, J.; Van Gils, S.; Beentjes, P. C. J.; Terryn, H.; de Wit, J. H. W. Ageing of Aluminium Oxide Surfaces and Their Subsequent Reactivity Towards Bonding with Organic Functional Groups. *Appl. Surf. Sci.* **2004**, *235*, 465–474.
- (31) Schoukens, J.; Pintelon, R.; Der Ouderaa, E. V.; Renneboog, J. Survey of Excitation Signals for FFT Based Signal Analyzers. *IEEE Trans. Instrum. Meas.* **1988**, *37*, 342–352.
- (32) Schoukens, J.; Pintelon, R.; Dobrowiecki, T. Linear Modeling in the Presence of Nonlinear Distortions. *IEEE Trans. Instrum. Meas.* **2002**, *51*, 786–792.
- (33) Smith, F. A.; Creitz, E. C. Infrared Studies of Association in Eleven Alcohols. *J. Res. Natl. Bur. Stand.* **1951**, *46*, 145–164.
- (34) Liddel, U.; Becker, E. D. Infra-red Spectroscopic Studies of Hydrogen Bonding in Methanol, Ethanol, and t-Butanol. *Spectrochim. Acta* **1957**, *10*, 70–84.
- (35) McInroy, A. R.; Lundie, D. T.; Winfield, J. M.; Dudman, C. C.; Jones, P.; Lennon, D. The Application of Diffuse Reflectance Infrared Spectroscopy and Temperature-Programmed Desorption to Investigate the Interaction of Methanol on  $\eta$ -alumina. *Langmuir* **2005**, *21*, 11092–11098.
- (36) Takezawa, N.; Kobayashi, H. The Shift of CH Stretching Band of Surface Alcoholate on Metal Oxides. *J. Catal.* **1972**, *25*, 179–181.
- (37) Van den Brand, J. On the Adhesion between Aluminium and Polymers. Ph.D. Dissertation, TU Delft: The Netherlands, 2004; p 239.
- (38) van den Brand, J.; Sloof, W. G.; Terryn, H.; de Wit, J. H. W. Correlation Between Hydroxyl Fraction and O/Al Atomic Ratio as Determined From XPS Spectra of Aluminium Oxide Layers. *Surf. Interface Anal.* **2004**, *36*, 81–88.
- (39) Van Gils, S.; Melendres, C. A.; Terryn, H. Quantitative Chemical Composition of Thin Films with Infrared Spectroscopic Ellipsometry: Application to Hydrated Oxide Films on Aluminium. *Surf. Interface Anal.* **2003**, *35*, 387–394.
- (40) Busca, G.; Lorenzelli, V. Infrared Study of Methanol, Formaldehyde, Adsorbed on Hematite. *J. Catal.* **1980**, *66*, 155–161.
- (41) Macía, L. F.; Petrova, M.; Hauffman, T.; Muselle, T.; Doneux, T.; Hubin, A. A Study of the Electron Transfer Inhibition on a Charged Self-Assembled Monolayer Modified Gold Electrode by Odd Random Phase Multisine Electrochemical Impedance Spectroscopy. *Electrochim. Acta* **2014**, *140*, 266–274.
- (42) Ozarem, M.; Tribollet, B. *Electrochemical Impedance Spectroscopy*; Wiley: New Jersey, 2008; Vol. 1.
- (43) de Laet, J.; Terryn, H. A.; Vereecken, J. The Use of Impedance Spectroscopy and Optical Reflection Spectroscopy To Study Modified Aluminium. *Electrochim. Acta* **1996**, *41*, 1155–1161.
- (44) Brug, G. J.; van den Eeden, A. L.; Sluyters-Rehbach, M.; Sluyters, J. H. The Analysis of Electrode Impedances Complicated by the Presence of a Constant Phase Element. *J. Electroanal. Chem. Interfacial Electrochem.* **1984**, *176*, 275–295.
- (45) O’Kane, D. F.; Mittal, K. L. Plasma Cleaning of Metal Surfaces. *J. Vac. Sci. Technol.* **1974**, *11*, 567–569.
- (46) Hajati, S.; Tougaard, S. Non-Destructive Depth Profiling by XPS Peak Shape Analysis. *J. Surf. Anal.* **2009**, *15*, 220–224.
- (47) McCafferty, E.; Wightman, J. P. Determination of the Concentration of Surface Hydroxyl Groups on Metal Oxide Films by a Quantitative XPS Method. *Surf. Interface Anal.* **1998**, *26*, 549–564.
- (48) Hauffman, T.; Hubin, A.; Terryn, H. Study of the Self-Assembling of n-Octylphosphonic Acid Layers on Aluminum Oxide from Ethanolic Solutions. *Surf. Interface Anal.* **2013**, *45*, 1435–1440.